Pergamon

Int. J. Heat Mass Transfer. Vol. 40, No. 7, pp. 1687–1692, 1997

0017-9310/97 $17.00+0.00

PII: S0017-9310(96)00200-1

Numerical study of heat transfer enhancement of a horizontal tube with an eccentrically inserted plate

C. I. HUNG and Y. S. LIN
Department of Mechanical Engineering, National Cheng Kung University, Tainan, Taiwan 70101, Republic of China

and

J. D. CHEN
E/E Section, Steel/Aluminium R&D Department, China Steel Corporation, Kaohsing, Taiwan, Republic of China

(*Received* 4 *January* 1996)

Abstract—A numerical study is presented for the heat transfer enhancement in a horizontal tube due to the insertion of an adiabatic plate. Special attention is placed on the effects of the eccentricity and tilted angle of the inserted plate on the heat transfer enhancement. The governing equations are first transformed into curvilinear coordinates, then discretized into the finite difference form through the finite-volume method. It is found that the greater the eccentricity, the smaller the pressure drop, and the worse the heat transfer effect. Also, the optimum position of the inserted plate is found to be at the center of the tube.

INTRODUCTION

The goal of enhancing the heat transfer capacity of thermal systems has led to the development of various research techniques. Such research can not only increase the operating efficiency of traditional heat exchangers, but can also result in significant energy savings. Most heat transfer enhancement technology can be categorized as being either active or passive depending on whether outside energy sources are needed [1]. It would be more economical if additional energy sources were not required for operation. In addition, most research on heat exchange system installation and operation, within the last decade, has centered on passive systems, most focused on finding optimal operation conditions and appropriate ranges for enhancing heat exchange.

Inserting a plate in a heat exchange tube is one type of simple passive heat exchange design. Shah and London [2] and Shah and Bhatti [3] provided a thorough review of the effects of this kind of heat exchange tube in laminar flows. Sastry [4] used the Schwarz–Neumann alternating method to investigate the forced convection in an annulus with a square core subjected to the fifth kind of thermal boundary condition. Cheng and Jamil [5] used the point matching technique to investigate the heat transfer for doubly connected ducts, under the conditions of axially uniform wall heat flux and circumferentially uniform wall temperature, at a given cross-section. Even though they provided a practical result for overall heat flow characteristics, their results showed negative speeds and shear stress, which are not physically reasonable. Solanki *et al.* [6, 7] studied laminar forced convection in tubes with polygonal inner cores; the Galerkin finite element method was used to obtain the numerical results. The number of sides was found to be an important factor. Chen [8] used the numerical method to study the laminar convection flow in a horizontal tube with a longitudinal rectangular inner core. His research work discussed the effects of: the width–height ratio of the plate, the radius ratio of the circumscribed circle to the plate to the tube, and the plate's horizontal and vertical eccentricity ratio, on heat flow characteristics. Manglik and Bergles [9] conducted an experimental study on heat transfer enhancement in horizontal tubes, with uniform wall temperatures, by means of twisted-tape insertion. Their results are strongly influenced by the tape geometry and the fluid flow condition.

In this work, a numerical method is used to analyze the laminar forced convection characteristics in a circular tube with an inserted adiabatic plate. In addition to investigating the effects of plate positioning on heat flow, this work also provides an estimation of the heat exchange effectiveness of an inserted plate in tubes—a discussion which has both theoretical and practical value.

NOMENCLATURE

AR	aspect ratio of plate, l/h
A_f	dimensionless flow area of the passage
A_f^*	dimensional flow area of the passage [m^2]
D_h	dimensionless hydraulic diameter, d_h/R_0
d_h	dimensional hydraulic diameter [m]
E	dimensionless center-to-center distance between plate and tube
dP/dZ	dimensionless axial pressure gradient
e_h, e_v	horizontal and vertical eccentricity [m]
fRe	friction factor–Reynolds number product
H	dimensionless height of the plate, h/R_0
h	local heat transfer coefficients [W m^{-2} K^{-1}]; height of the plate [m]
J	Jacobian of the transform
k	thermal conductivity of fluid [W m^{-1} K^{-1}]
L	dimensionless width of plate, l/R_0
l	dimensional width of plate [m]
N	dimensionless normal direction
Nu	Nusselt number
$\bar{P}$	dimensional fluid pressure [N m^{-2}]
PE	normalized pressure drop, see equation (14)
PL	normalized peripheral location along the plate, $(\xi-\xi_{min})/(\xi_{max}-\xi_{min})$
P_0^*	dimensional perimeter of tube [m]
P_0	dimensionless perimeter of tube
QE	normalized heat transfer rate, see equation (13)
q''_{in}	axial uniform heat flux input on tube [W m^{-2}]
Q_p	normalized overall heat transfer rate per unit pumping power, see equation (15)
R_0	radius of tube [m]
RR	radius ratio of the circumscribed circle of plate to the tube, $0.5(L^2+H^2)^{0.5}$
T	dimensionless temperature
t	dimensional temperature [K]
W	dimensionless axial velocity
w	dimensional axial velocity [m s^{-1}]
X, Y	dimensionless coordinate system
x, y	dimensional coordinate system [m].

Greek symbols

α, β, γ	transformation coefficients
δ	tilted angle of plate
θ	angular position
μ	dynamic viscosity of fluid [N s m^{-2}]
ξ, η	dimensionless coordinates in the transformed domain
ρ	fluid density [kg m^{-3}]
τ	overall wall shear stress [N m^{-2}].

Subscripts

b	bulk value
bare	value of bare tube
m	mean value
max	maximum value
min	minimum value
s	surface value.

THEORETICAL ANALYSIS

The physical model of a heat exchange tube with an inserted plate is presented in Fig. 1. In this work, the tube is assumed to have axially uniform heat flux q''_{in} with a peripherally uniform temperature. The inserted plate is abiabatic so as to place emphasis on the change of flow field and the consequent heat transfer alternation. They physical properties of the fluid are taken as constants. The flow is considered to be steady, laminar and fully developed. The dimensionless variables are given in the following, defined as:

$$X=\frac{x}{R_0} \quad Y=\frac{y}{R_0} \quad Z=\frac{zD_h}{R_0R_e} \quad D_h=\frac{d_h}{R_0}$$

$$A_f=\frac{A_f^*}{R_0^2} \quad P_0=\frac{P_0^*}{R_0^2} \quad W=\frac{w}{w_m} \quad w_m=\frac{R_0^2}{\mu}$$

$$T=\frac{t-t_s}{q''_{in}R_0/k} \quad \bar{P}=\frac{\bar{p}}{\rho w_m^2} \quad R_e=\frac{w_m d_h}{\nu}.$$

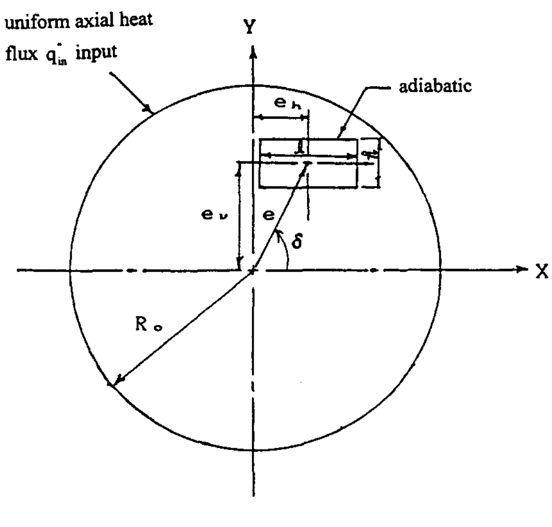

Fig. 1. Physical model of a heat exchange tube with an inserted plate.

Based on the above assumptions, the dimensionless governing equations can be formulated as

$$\frac{\partial^2 W}{\partial X^2}+\frac{\partial^2 W}{\partial Y^2}-\frac{d\bar{P}}{dZ}=0 \tag{1}$$

$$\frac{\partial^2 T}{\partial X^2}+\frac{\partial^2 T}{\partial Y^2}-W\frac{P_0}{A_f}=0. \tag{2}$$

The associated boundary conditions are

$$\text{at the inner wall:}\quad W=0 \quad \frac{\partial T}{\partial N}=0 \tag{3}$$

$$\text{at the outer wall:}\quad W=0 \quad T=0. \tag{4}$$

In the fully developed condition, the axial pressure gradient $\partial\bar{P}/\partial Z$ should be a constant. Therefore, we can incorporate this axial pressure gradient term into the dimensionless axial velocity, W', by defining

$$W'=\frac{W}{-d\bar{P}/dZ}. \tag{5}$$

With this definition, equations (1) and (2) can be rewritten as:

$$\frac{\partial^2 W'}{\partial X^2}+\frac{\partial^2 W'}{\partial Y^2}+1=0 \tag{6}$$

$$\frac{\partial^2 T}{\partial X^2}+\frac{\partial^2 T}{\partial Y^2}-\frac{W'}{W'_m}\frac{P_0}{A_f}=0. \tag{7}$$

At this point, the superscript of axial speed '′' can be ignored to simplify the symbols. In this work, we use the body-fitted coordinate system [10], to transfer the irregular physical domain into regular computational domain before initiating calculations. The coordinate (ξ,η) must satisfy a set of elliptic partial differential equations; the Thomas method [11], is used to place grid lines more densely on the solid walls with more physical activity and to construct a non-orthogonal network. After transformation, the governing equations become

$$\frac{\partial}{\partial\xi}\left(\frac{\alpha}{J}\frac{\partial W}{\partial\xi}-\frac{\beta}{J}\frac{\partial W}{\partial\eta}\right)+\frac{\partial}{\partial\eta}\left(\frac{\gamma}{J}\frac{\partial W}{\partial\eta}-\frac{\beta}{J}\frac{\partial W}{\partial\xi}\right)+J=0 \tag{8}$$

$$\frac{\partial}{\partial\xi}\left(\frac{\alpha}{J}\frac{\partial T}{\partial\xi}-\frac{\beta}{J}\frac{\partial T}{\partial\eta}\right)+\frac{\partial}{\partial\eta}\left(\frac{\gamma}{J}\frac{\partial T}{\partial\eta}-\frac{\beta}{J}\frac{\partial T}{\partial\xi}\right)-J\frac{WP_0}{W_mA_f}=0 \tag{9}$$

in which

$$\alpha=X_\eta^2+Y_\eta^2$$
$$\beta=X_\xi X_\eta+Y_\xi Y_\eta$$
$$\gamma=X_\xi^2+Y_\xi^2$$
$$J=X_\xi Y_\eta-X_\eta Y_\xi.$$

Equations (8) and (9) are discretized via the finite-volume method. The SIMPLE algorithm [12] in Cartesian coordinates is extended to the body-fitted coordinate system. The pressure correction equation is derived following the procedure of Shyy *et al.* [13]. The resulting difference equations are then solved iteratively line-by-line, with over-relaxation to accelerate the convergence. In this work, the over-relaxation factor for each variable is chosen as 1.7. The criterion for convergence is chosen as $|(\phi^n-\phi^{n-1})/\phi^n|<10^{-5}$, $\phi=W$ or T, for each node.

In the discussion on heat flow characteristics in this work, the friction factor-Reynolds number product fRe, and the local and cross-sectional average Nusselt numbers Nu and Nu_m, are defined, respectively, as:

$$fRe=\frac{\tau}{\frac{1}{2}\rho w_m^2}\frac{\rho w_m d_h}{\mu}=\frac{D_h^2}{2}\left(-\frac{d\bar{P}}{dZ}\right) \tag{10}$$

$$Nu=\frac{hd_h}{k}=\left(\frac{\partial T}{\partial N}\right)_s\frac{D_h}{T_b} \tag{11}$$

$$Nu_m=\frac{h_m d_h}{k}=-\frac{D_h}{T_b}. \tag{12}$$

In evaluating the effectiveness of enhancing the performance of heat exchange, the evaluation principle proposed by Lau *et al.* [14] which is well-suited to numerical studies, is used. In this evaluation criterion, the normalized heat transfer rate QE, the normalized pressure drop, PE, and the normalized overall heat transfer rate per unit pumping power Q_p, are defined as:

$$QE=-\frac{q''_{in}/(t_s-t_b)}{(Nu_m)_{bare}k/(d_h)_{bare}}=-\frac{0.4587}{T_b} \tag{13}$$

$$PE=\frac{fRe}{(fRe)_{bare}}\frac{(d_h^2)_{bare}}{d_h^2}\frac{w_m}{(w_m)_{bare}}=\frac{fRe}{4D_h^2}\frac{\pi}{A_f} \tag{14}$$

$$Q_p=\frac{QE}{PE^{1/3}}=-\frac{0.4972}{T_b}\left(\frac{D_h^2A_f}{fRe}\right)^{1/3}. \tag{15}$$

Here, $Q_p\geqslant 1$ represents the net positive enhancement effect, and $Q_p<1$ represents the net negative effect.

RESULTS AND DISCUSSION

This work investigates the effects of an eccentrically inserted plate, inside a horizontal tube, on the heat transfer character and the optimal positioning of the plate. Special attention is placed on the effects of the eccentricity, E, and the tilted angle of the inserted plate, δ, on the heat transfer enhancement. To test the effect of grid refinement on numerical solutions, we choose a test case with $AR=2.0$ and $RR=0.5$, where AR is the aspect ratio of the plate and RR is the radius ratio of the circumscribed circle of the plate to the tube. Three uniform grid systems, 44×25, 74×36, 92×44, are used in a computational domain. As

Table 1. Results of grid test ($AR = 2.0, RR = 0.5$)

$NX \times NY$	fRe	Nu_m
44×28	22.68	4.549
74×36	22.35	4.460
92×44	22.37	4.471

shown in Table 1 the discrepancy between the first two grids is greater than 1% while for the next two grids the discrepancy is less than 0.26%. Therefore, the 74×36 grid was used in all calculations. The results of fRe values in this research and in the previous study [2], in regard to concentric square plate insertion, are compared and shown in Fig. 2. The results indicate that the calculation method used in this research is highly reliable.

In this investigation, the eccentricity of the plate, E, was selected to be 0.0, 0.1, 0.2, 0.3, 0.4 and 0.5. The tilted angle, δ, which means that the center-to-center line of the plate and the tube was aligned with the x-axis, is chosen as 0, 30, 60 and 90 degrees. Through these parameter variations, we can understand the detailed change of the heat transfer characteristics. To focus on the effects of plate positioning on heat transfer, a plate with aspect ratio $AR = 1.25$ and radius ratio $RR = 0.5$ was established.

For the sake of brevity, only the plots of $E = 0.5$ are presented here. Other results can be found in ref. [15]. Figure 3 shows the effect of tilted angle on the flow field and heat transfer for $E = 0.5$, $AR = 1.25$ and $RR = 0.5$. The case of $\delta = 0$ has right-hand horizontal eccentricity. Due to this eccentricity, the clearance on the right-hand side of the plate is smaller, and this causes greater flow resistance and hence, a resulting lower flow rate. This is called the pressure side. The effect is opposite on the left-hand side, and hence it is called the expansion side. In addition, under the wall conditions of externally uniform temperature and internally adiabatic boundary, the fluid temperature would be highest at the outside wall. Regardless of the position of the plate, due to the lower flow rate in the pressure side, the temperature gradient is always smaller in the pressure side; as a result, heat distribution in the pressure side is relatively uniform and high.

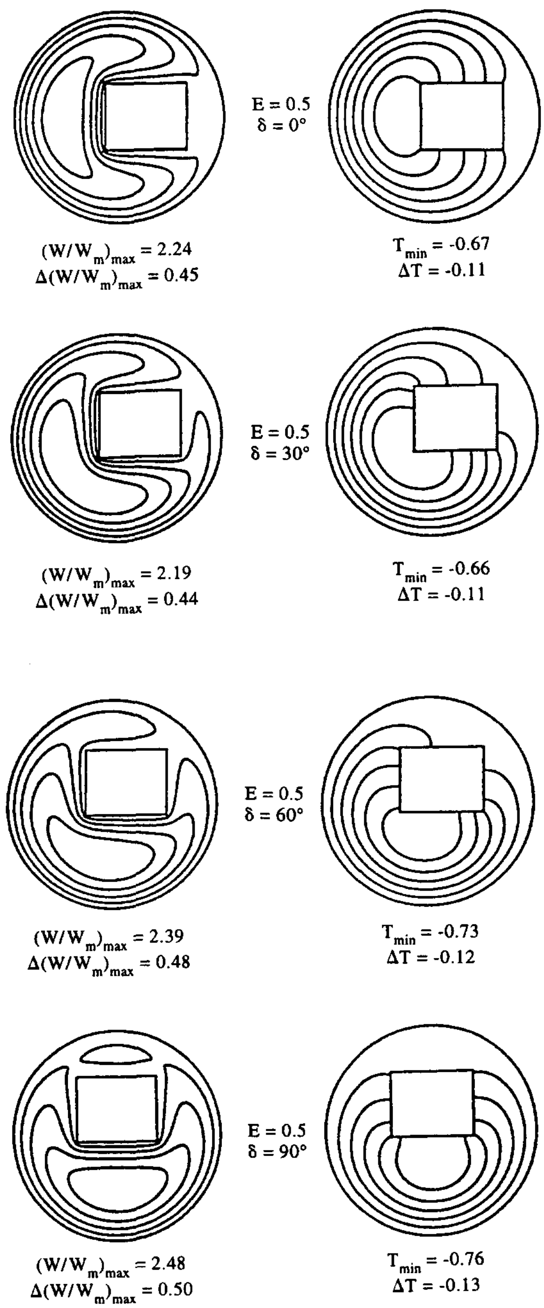

Fig. 3. Effects of tilted angle of inserted plate on flow field and isotherms, $E = 0.5$, $AR = 1.25$ and $RR = 0.5$.

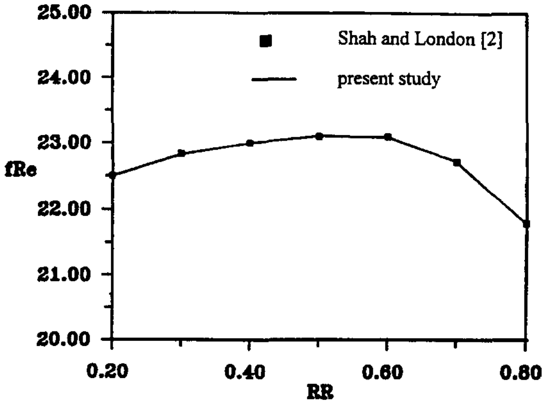

Fig. 2. Comparison of fRe for the case of concentric square core.

Figure 4 shows the tilted angle effect on the distribution of peak axial speed of each cross-section at a point along the surface of inserted plate. The parameter PL, the normalized peripheral position along the plate, starts from the center point on the upper surface. Due to the fact that the plate is eccen-

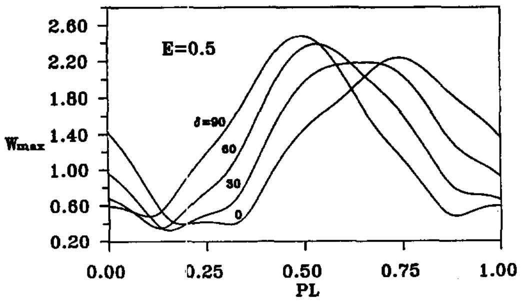

Fig. 4. Distribution of cross-sectional peak speed along the inserted plate under the variation of tilted angle, for $E = 0.5$.

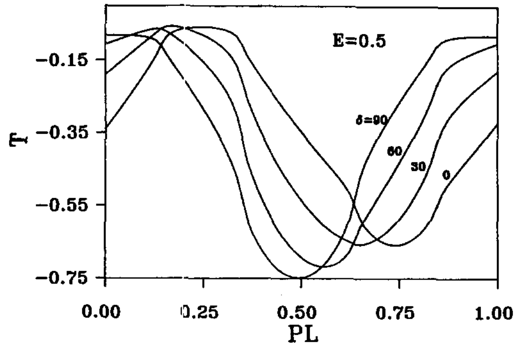

Fig. 5. Circumferential temperature distribution of inserted plate, $E = 0.5$.

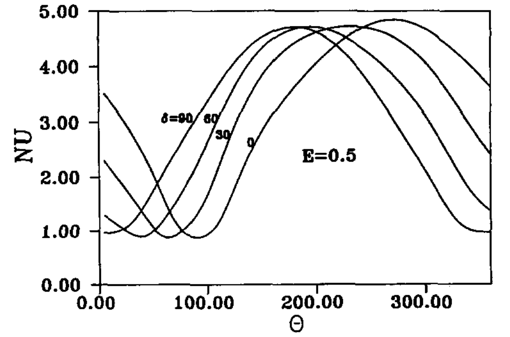

Fig. 6. Distribution of tubeside local Nusselt number, $E = 0.5$.

Table 2. Evaluation of the effect of plate positioning on heat transfer characteristics

E	δ(o)	fRe	Nu_m	PE	QE	Q_p
0.0		23.03	4.782	5.0027	1.8791	1.0987
0.1	0	22.82	4.669	4.9571	1.8348	1.0761
	30	22.81	4.656	4.9549	1.8297	1.0732
	60	22.80	4.629	4.9527	1.8195	1.0674
	90	22.80	4.616	4.9507	1.8138	1.0641
0.2	0	22.23	4.375	4.8289	1.7193	1.0172
	30	22.21	4.331	4.8246	1.7020	1.0073
	60	22.16	4.247	4.8137	1.6692	0.9886
	90	22.14	4.206	4.8094	1.6530	0.9793
0.3	0	21.31	3.997	4.6291	1.5709	0.9426
	30	21.27	3.926	4.6204	1.5429	0.9263
	60	21.18	3.789	4.6100	1.4893	0.8954
	90	21.13	3.724	4.5900	1.4632	0.8804
0.4	0	20.16	3.622	4.3723	1.4237	0.8702
	30	20.09	3.535	4.3641	1.3892	0.8501
	60	19.95	3.367	4.3336	1.3230	0.8115
	90	19.88	3.287	4.3184	1.2917	0.7932
0.5	0	18.86	3.268	4.0969	1.2947	0.8091
	30	18.76	3.202	4.0752	1.2584	0.7879
	60	18.57	3.024	4.0339	1.1883	0.7465
	90	18.48	2.939	4.0143	1.1548	0.7266

trically shifted in the counter clockwise direction, the flow clearance increases, and the flow rate and the peak speed also increase in the region of $PL = 0.2$–0.5. In contrast, when $PL = 0.7$–1.0, because the flow clearance is decreased, the flow rate and peak speeds are also decreased.

Figure 5 shows the temperature distribution along the surface of the inserted plate. A comparison of Figs. 4 and 5 shows that there is an inverse relationship between the circumferential temperature distribution and the cross-sectional flow rate distribution. When δ increases from 0–90 degrees and PL is in the approximate range of 0.25–0.5, the plate surface temperatures decrease with the increase of flow rates. When PL is approximately between 0.7 and 1.0, the opposite trend occurs. The highest temperature appeared on the right side for $\delta = 0°$. When $\delta = 90°$, the highest temperature was found on the upper surface of the plate. For other positionings, the highest temperatures were found on the upper right-hand side of the plate (i.e. $PL < 0.25$, approximately).

The circumferential distribution of the Nusselt numbers on the tube side is shown in Fig. 6. In general, the Nusselt number increases with an increase in the flow rate. In changing from $\theta = 0°$ to $\theta = 90°$, which approaches the pressure side, flow rates dropped and the Nusselt number decreased; the lowest values were found. In leaving the pressure side, flow rates decreased and the Nusselt number gradually increased. At, $\theta \geqslant 200°$, which is far from the expansion side, the flow rates dropped and the Nusselt number decreased correspondingly.

Finally, Lau's principle [14] was used to evaluate the effect of plate positioning on heat transfer characteristics. As listed in Table 2, the results show that eccentric plate insertion helps decrease fluid pressure drop, but also decreases the heat transfer. This disadvantage far outweighs the benefit of the former, it causes the net heat transfer effect to drop as the eccentricity of the position increases; as a result, concentric positioning works best in enhancing heat transfer.

CONCLUSION

In the present study, the heat transfer enhancement of a horizontal tube, with an eccentricly inserted adiabatic plate subjected to axially uniform heat flux input and circumferentially uniform wall temperature, is studied numerically. Special attention is placed on the effects of the eccentricity and the tilted angle of the inserted plate on the heat transfer enhancement. From this thorough investigation into optimal plate positioning, the following conclusions can be drawn:

(1) The circumferential distribution of the Nusselt number has a direct positive correlation with the cross-sectional flow rate distribution.

(2) With the same cross-sectional flow rates, eccentric placement causes more of a reduction in fluid pressure drop than concentric placement, but also reduces heat transfer enhancement.

(3) In the eccentric position, with an eccentricity E, the larger the tilted angle δ, the less the pressure drop. This causes the Nu_m to drop and hence, the heat transfer enhancement is decreased.

REFERENCES

1. Bergles, A. E., Techniques to augment heat transfer. In *Handbook of Heat Transfer Application*, 2nd ed., Chap. 3, ed. W. M. Rohsenow, J. P. Hartnett and E. N. Ganis. McGraw-Hill, New York, 1985.
2. Shah, R. K. and London, A. L., Laminar flow forced convection in ducts. Supplement 1 to *Advances in Heat Transfer*. Academic Press, New York, 1978.
3. Shah, R. K. and Bhatti, M. S., Laminar convective heat transfer in ducts. In *Handbook of Single-Phase Convective Heat Transfer*, Chap. 3, Ed. S. Kakac, R. K. Shah and W. Aung. Wiley, New York, 1987.
4. Sastry, U. A., Heat transfer by laminar force convection in multiply-connected regions. *Acta Technika (Budapest)*, 1965, **51,** 181–192.
5. Cheng, K. C. and Jamil, M., Laminar flow and heat transfer in circular ducts with diametrically opposite flat sides and ducts of multiply connected cross sections. *Canadian Journal of Chemical Engineering*, 1970, **48,** 333–334.
6. Solanki, S. C., Saini, J. S. and Gupta, C. P., Flow through doubly connected ducts. *International Journal of Heat & Fluid Flow*, 1986, **7,** 301–306.
7. Solanki, S. C., Prakash, S., Saini, J. S. and Gupta, C. P., Forced convection heat transfer in doubly connected ducts. *International Journal of Heat & Fluid Flow*, 1987, **8,** 107–110.
8. Chen, J. D., A study on efficiency promotion of the crossflow type tubular heat exchanger. Ph.D. dissertation, National Sun Yat-Sen University, Kaohsiung, Taiwan, 1991.
9. Manglik, R. M. and Bergles, A. E., Heat transfer enhancement and pressure drop in viscous liquid flows in isothermal tubes with twisted-tape inserted. *Warme- und Stoffubertragung*, 1992, **27,** 249–257.
10. Thompson, J. F., Thames, F. C. and Marsin, C. W., Automatic numerical generation of body-fitted curvilinear coordinate system for field containing any number of arbitrary two-dimensional bodies. *Journal of Computational Physics*, 1974, **15,** 299–319.
11. Thomas, P. D. and Middlecoff, J. F., Direct control of the grid point distribution in meshes generated by elliptic equations. *AIAA Journal*, 1980, **18,** 652–656.
12. Patankar, S. V., *Numerical Heat Transfer and Fluid Flow*. Hemisphere, New York, 1980.
13. Shyy, W., Tong, S. S. and Correa, S. M., Numerical recirculating flow calculation using a body-fitted coordinate system. *Numerical Heat Transfer*, 1985, **8,** 99–113.
14. Lau, S. S., Ong, L. E. and Han, J. C., Conjugate heat transfer in channels with internal longitudinal fins. *Journal of Thermophysics & Heat Transfer*, 1989, **3,** 303–308.
15. Lin, Y. S., Study on heat transfer enhancement of horizontal tube with an inserting plate. M.Sc. thesis, Department of Mechanical Engineering, National Cheng-Kung University, Tainan, Taiwan, 1982.